Joint Diseases and Related Surgery

Jt Dis Relat Surg
2026;37(x):i-xi

ORIGINAL ARTICLE

Effects of proximal fibular osteotomy on tibiofibular and medial knee loads in severe varus: A finite element study

Oğuzhan Pekince, Ahmet Yıldırım

Department of Orthopedics and Traumatology, Konya City Hospital, Konya, Türkiye

ABSTRACT

Objectives: This study aims to evaluate the biomechanical effects of proximal fibular osteotomy (PFO) on tibiofemoral and proximal tibiofibular load transfer under simulated neutral and varus alignment conditions using a lower-extremity finite element analysis (FEA) model.

Materials and Methods: A patient-specific three-dimensional FEA model of the lower extremity was developed from computed tomography and magnetic resonance imaging data of a healthy volunteer. Neutral, 3° varus, and 5° varus alignments were simulated before and after PFO under a simplified physiological axial load of 900 N. Tibiofemoral compartment forces, proximal tibiofibular joint (PTFJ) force, distal tibiotalar reaction force, and peak von Mises stresses within the cartilage-meniscus complex were evaluated.

Results: Proximal fibular osteotomy markedly reduced PTFJ force across all alignment conditions. Under neutral alignment, PTFJ force decreased from 122.94 N to 21.84 N, while distal tibiotalar reaction force increased from 787.55 N to 897.89 N, indicating redistribution of load through distal pathways. Tibiofemoral compartment forces changed minimally. Under 5° varus alignment, medial tibiofemoral force decreased only from 608.45 N to 603.78 N following PFO. Peak medial meniscal and cartilage stresses increased with varus alignment and remained largely unchanged after osteotomy.

Conclusion: In this single-subject static FEA model, PFO substantially reduced proximal tibiofibular loading, but produced only limited changes in tibiofemoral load distribution under simulated varus alignment. Within the present model, load redistribution occurred predominantly through distal load-transfer pathways rather than substantial unloading of the medial tibiofemoral compartment. These findings suggest that the biomechanical effect of PFO may primarily involve alteration of fibular load transmission rather than meaningful reduction of medial knee loading.

Keywords: Biomechanics, finite element analysis, genu varum, knee joint, osteotomy, tibiofibular joint.

Proximal fibular osteotomy (PFO) has gained increasing interest as a minimally invasive option for medial compartment knee osteoarthritis (OA) in patients with varus malalignment. The procedure is mechanistically grounded in the "non-uniform settlement" and "too many cortices" theories, which propose that disrupting lateral column support through fibular resection facilitates load redistribution away from the overloaded medial tibiofemoral compartment.[1,2] In line with this rationale, clinical studies have reported favorable short-term outcomes following PFO, including pain relief, increased medial joint space, and improved functional scores in varus-aligned osteoarthritic knees.[3]

Despite these promising findings, the broader biomechanical implications of fibular resection remain incompletely understood. The fibula is not merely a passive lateral stabilizer of the knee, but an integral component of the lower extremity load-bearing apparatus, contributing to force transmission through the proximal tibiofibular joint (PTFJ) and the interosseous membrane. Consequently, disruption of fibular integrity may exert biomechanical effects that extend beyond simple lateral column unloading,

Received: May 23, 2026
Accepted: July 02, 2026
Published online: July 16, 2026

Correspondence: Oğuzhan Pekince, MD. Konya Şehir Hastanesi, Ortopedi ve Travmatoloji Anabilim Dalı, 42020 Karatay, Konya, Türkiye.

E-mail: oguzhanpekince@hotmail.com

Doi: 10.52312/jdrs.2026.2965

Citation: Pekince O, Yıldırım A. Effects of proximal fibular osteotomy on tibiofibular and medial knee loads in severe varus: A finite element study. Jt Dis Relat Surg 2026;37(x):i-xi. doi: 10.52312/jdrs.2026.2965.

with potential implications for load distribution across the tibiofemoral joint and the proximal tibiofibular articulation.

Recent finite element analysis (FEA) studies have demonstrated reductions in medial compartment loading following PFO.[4,5] However, most of these investigations are limited by the use of isolated knee models, low-magnitude static loading conditions, and a single alignment scenario, typically neutral or mildly varus. Such simplifications may fail to capture the complex load transfer mechanisms involving the menisci and the PTFJ, particularly under more demanding mechanical conditions such as severe varus malalignment.

Under physiological loading conditions, the fibula contributes to interosseous membrane tension and load transmission patterns within the lower extremity.[6] Therefore, evaluating the effects of physiologically relevant, high-magnitude axial loads, such as the approximately 900 N encountered during the stance phase of gait, across a range of varus alignments is essential for accurately characterizing the biomechanical impact of PFO and identifying the conditions under which its unloading capacity may become insufficient.

In the present study, we aimed to investigate the biomechanical effects of PFO on tibiofemoral load distribution and PTFJ mechanics across neutral and simulated varus alignments using a three-dimensional (3D) FEA model of the lower extremity paying particular attention toward load redistribution within the meniscus-cartilage complex and the PTFJ under a physiologically relevant 900 N axial load, and to determine whether the biomechanical influence of PFO extended beyond local fibular unloading to alter overall tibiofemoral load transfer as varus deformity progresses.

MATERIALS AND METHODS

Construction of the three-dimensional finite element model

This computational biomechanical study using FEA was conducted at Konya City Hospital, Department of Orthopedics and Traumatology between January 2026 and April 2026. A patient-specific 3D FEA model of the lower extremity was developed using computed tomography (CT) and magnetic resonance imaging (MRI) data obtained from a healthy 33-year-old male volunteer (90 kg) without known knee OA.

Computed tomography data of the right lower extremity were acquired using a multidetector CT scanner (Revolution EVO, GE Medical Systems, USA). Imaging was performed with a tube voltage of 120 kV and a tube current of 80 mA. Axial images were reconstructed using a standard bone reconstruction algorithm with a matrix size of 512 × 512 pixels and a field of view of 325 mm, resulting in an in-plane pixel resolution of approximately 0.63 mm. A total of 837 axial slices were obtained with a slice thickness and slice increment of 0.625 mm, without gantry tilt. The acquired dataset included the distal femur, tibia, fibula, talus, and calcaneus and was exported in Digital Imaging and Communications in Medicine (DiCOM) format for segmentation and three-dimensional reconstruction.

Magnetic resonance imaging data were acquired using a 1.5-T clinical MRI scanner (MAGNETOM Sempra, Siemens Healthineers, Erlangen, Germany) with an extremity coil. A proton density-weighted turbo spin echo fat-suppressed sagittal sequence (PD-TSE FS SAG) was used for segmentation of cartilage, menisci, and ligament attachment regions. Imaging parameters included a repetition time (TR) of 2670 ms, an echo time (TE) of 28 ms, a flip angle of 160°, and a slice thickness of 3.5 mm. Images were acquired with a matrix size of 576 × 576 pixels and an in-plane resolution of 0.3125 × 0.3125 mm. The MRI data were exported in DiCOM format and processed for anatomical segmentation and soft tissue reconstruction.

The CT datasets were used to reconstruct the osseous structures, including the distal femur, tibia, fibula, talus, and calcaneus, whereas articular cartilage and menisci of the knee joint were segmented from MRI data. Segmentation was performed using semi-automatic techniques combined with manual anatomical refinement in 3D Slicer (version 5.6.2). Particularly in cartilage surfaces, menisci, and ligament attachment regions, anatomical accuracy was prioritized over fixed threshold-based segmentation alone. Surface smoothing and mesh repair procedures were performed in Autodesk Meshmixer prior to solid model generation. The resulting geometries were subsequently imported into SolidWorks 2018 (Dassault Systèmes, Vélizy-Villacoublay, France) for assembly and anatomical alignment.

To ensure a physiologically representative model, major ligamentous structures of both the knee and ankle were incorporated. These included the anterior and posterior cruciate ligaments, medial and lateral collateral ligaments, distal tibiofibular syndesmotic ligaments, and primary stabilizers of the ankle joint. All ligamentous structures were modeled as tension-only linear spring elements, consistent with previous FEA studies,[4,6] and a uniform pre-strain of 2% was applied to all ligament structures.

A comprehensive overview of the constructed model is presented in Figure 1, and the incorporated ligamentous structures along with their corresponding stiffness values are summarized in Table I.

Material properties and mesh generation

All anatomical components in the model were assigned linear elastic, homogeneous, and isotropic material properties based on well-established values reported in the literature. The elastic modulus was defined as 17,000 MPa for cortical bone and 700 MPa for cancellous bone, both with a Poisson's ratio of 0.3. The menisci and articular cartilage were assigned elastic moduli of 80 MPa and 12 MPa, respectively.[6] Material properties for all model components are summarized in Table II.

The solid model was discretized using four-node linear tetrahedral elements, selected for their computational efficiency and robust performance in complex anatomical geometries involving multiple contact interfaces. An average element size of 3 mm was applied to osseous structures, while a refined mesh size of 0.5 mm was used for the cartilage, menisci, and contact interfaces, where higher stress gradients were expected. This element type is widely used in orthopedic FEA studies owing to its stability in large-scale contact analyses and compatibility with automated meshing of irregular biological structures.

A mesh convergence analysis was performed using progressively refined tetrahedral meshes to ensure solution independence from mesh density. The convergence assessment was based on three representative biomechanical parameters: medial tibiofemoral contact force, PTFJ force, and maximum meniscal stress. Mesh convergence analysis was performed under the same 900 N axial loading condition used in all final simulations to ensure direct comparability between convergence assessment and reported biomechanical outcomes. Convergence was considered achieved when variations in medial contact force, proximal tibiofibular force, and maximum meniscal stress remained below 5%

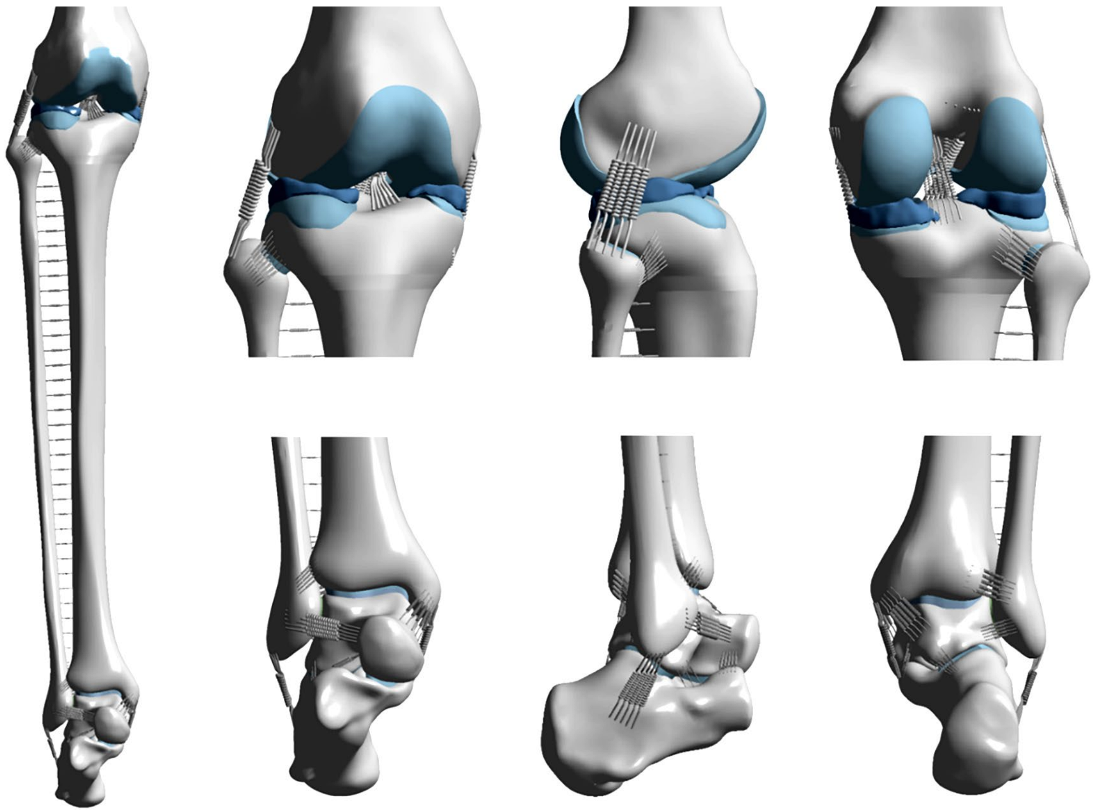

FIGURE 1. Patient-specific finite element model of the lower extremity including three-dimensional bony and soft-tissue geometries and one-dimensional tension-only ligament elements.

TABLE I
Ligament definitions and stiffness values used in the finite element model

Ligament	Stiffness (N/mm)
Anterior tibiotalar	70
Posterior tibiotalar	80
Tibiocalcaneal	120
Cervical	70
Lateral talocalcaneal	70
Posterior talocalcaneal	70
Medial talocalcaneal	70
Interosseous talocalcaneal	70
Calcaneofibular	70.5
Posterior talofibular	39.8
Anterior talofibular	39.9
Interosseous membrane	224.2
Interosseous ligament	224.2
Posterior inferior tibiofibular	101
Anterior inferior tibiofibular	78
Anterior superior tibiofibular	133
Posterior superior tibiofibular	109
Anterior cruciate ligament	200
Posterior cruciate ligament	200
Medial collateral ligament	100
Lateral collateral ligament	100

between successive refinements (Table III). As the final two refinements produced changes below 1% for all monitored parameters, the mesh containing 736,669 elements and 154,763 nodes was selected for all subsequent analyses as an optimal balance between numerical stability and computational efficiency.

Simulation of proximal fibular osteotomy and varus deformity

Proximal fibular osteotomy was simulated by virtually removing a 10-mm fibular segment approximately 60 mm distal to the fibular head, creating a non-contact osteotomy gap and reducing the structural support of the lateral column. The osteotomy level was selected to remain distal to the commonly described safe zone of the common peroneal nerve.[2,3] Different osteotomy levels were not separately simulated in the present study, as previous FEAs by Kang et al.[4] reported no substantial biomechanical differences in medial compartment stress redistribution among proximal, middle, and distal fibular osteotomy levels.

To evaluate the biomechanical effects of PFO under varying coronal plane alignments, varus deformities of 3° and 5° were introduced in both intact and osteotomy models. Simulated varus alignment was introduced by rotating the tibia

TABLE II
Material properties assigned to model components

Material	Modulus of elasticity (MPa)	Poisson's ratio
Cortical bone	17000	0.3
Cancellous bone	700	0.3
Menisci	80	0.3
Cartilage tissue	12	0.42

MPa, Megapascal.

TABLE III
Mesh convergence analysis under 900 N axial loading

Elements	Medial force (N)	PTFJ force (N)	Max meniscus stress (MPa)
426122	496.73	122.32	6.91
566680	505.92	123.91	7.36
656042	516.12	121.33	7.71
736669	**519.11**	**122.94**	**7.96**
833881	519.89	123.19	8.02

PTFJ, proximal tibiofibular joint; MPa, Megapascal.

relative to the femur around the anteroposterior axis passing through the center of the knee joint, thereby reproducing clinically relevant coronal plane malalignment conditions.

Simplified boundary conditions and physiological loading scenario

All FEAs were performed using ANSYS Workbench (ANSYS Inc., Canonsburg, PA, USA). A coefficient of friction of 0.2 was assigned between the femoral cartilage and menisci and between the femoral and tibial cartilage surfaces, whereas all other articulations were defined as frictionless, in line with previous modeling studies.[7] The applied boundary conditions and loading configuration are illustrated in Figure 2.

To reproduce a simplified weight-bearing loading condition, the inferior surface of the calcaneus was fully constrained in all degrees of freedom. The talus was restricted in the anteroposterior direction to prevent non-physiological translational motion while preserving vertical load transmission. The fibula was left unconstrained, allowing load transfer through the fibular column.

A vertical compressive load of 900 N, representing a simplified physiologically relevant axial loading condition during single-limb stance, was applied to the proximal femur along the mechanical axis.

Since the model included multiple contact interfaces, ligament constraints, and distal boundary reactions, externally applied loads were distributed across the entire lower-extremity system rather than exclusively through tibiofemoral contact forces. Therefore, reductions observed at a specific interface (e.g., PTFJ force after PFO) were not expected to appear as equivalent increases in medial or lateral tibiofemoral contact force. To verify preservation of global force equilibrium following osteotomy, distal tibiotalar reaction forces were additionally recorded and evaluated together with tibiofemoral and proximal tibiofibular reaction forces.

Static structural analyses were performed using ANSYS Workbench 2021 R2. Contact formulations, friction coefficients, boundary conditions, and loading scenarios were defined as described above. Peak von Mises stress distributions within the menisci and tibiofemoral articular cartilage were recorded as primary outcome measures.

Model verification and validation

Mesh convergence was assessed based on the criterion that variations in primary outcome measures remained below 5% with successive mesh refinements.[5,7] The final mesh of the reference intact model consisted of 154,763 nodes and 736,669 elements.

A compressive load of 900 N, derived from the volunteer's body weight of 90 kg assuming single-limb stance conditions, was applied to the proximal femur along the mechanical axis.[4,7] The modeling parameters, including ligament stiffness values, contact definitions, and boundary conditions, were adopted from previously published FEA studies of the lower extremity.[4,6,7] Model credibility was supported through numerical convergence assessment and consistency of predicted load-transfer patterns with the prescribed boundary conditions. However, no cadaveric or *in vivo* experimental validation was performed. Furthermore, the analysis was based on a single healthy volunteer and therefore does not represent interindividual anatomical variability or pathological tissue conditions. Consequently, the present model should be interpreted as a comparative numerical framework intended

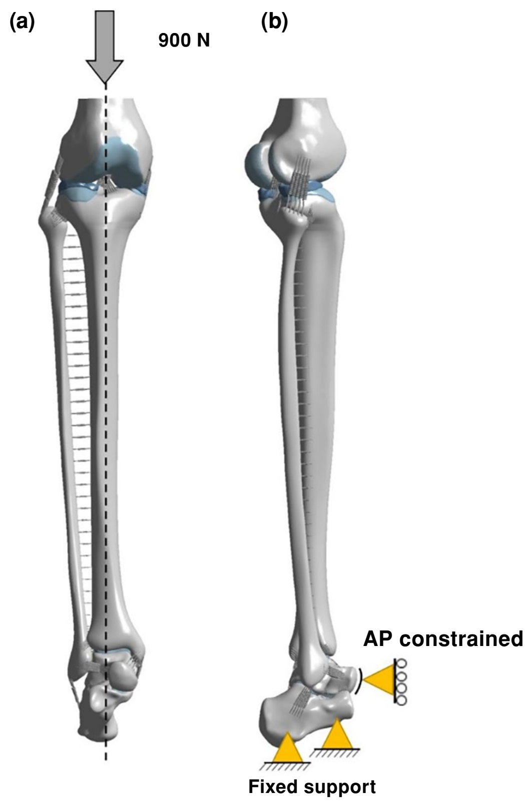

FIGURE 2. Loading and boundary conditions used in the simulations: **(a)** application of a 900 N axial compressive load along the mechanical axis; **(b)** distal constraints with fixed calcaneal support and anterior-posterior restriction of the talus.

AP, anteroposterior.

to identify relative biomechanical trends rather than reproduce absolute subject-specific *in vivo* mechanics.

Statistical analysis

In the statistical analysis of the study, contact stress, reaction force, and proximal tibiofibular joint force values obtained from each finite element simulation scenario were recorded and compared descriptively across the different alignment conditions. The results were presented in tables and figures. Since this was a deterministic finite element simulation study, classical parametric or non-parametric hypothesis tests were not applied, and the findings were reported as numerical outputs generated from the computational model.

RESULTS

Tibiofemoral load distribution and proximal tibiofibular joint kinetics

Under a physiological axial load of 900 N, both simulated varus alignment and PFO produced distinct effects on tibiofemoral load distribution and PTFJ mechanics.

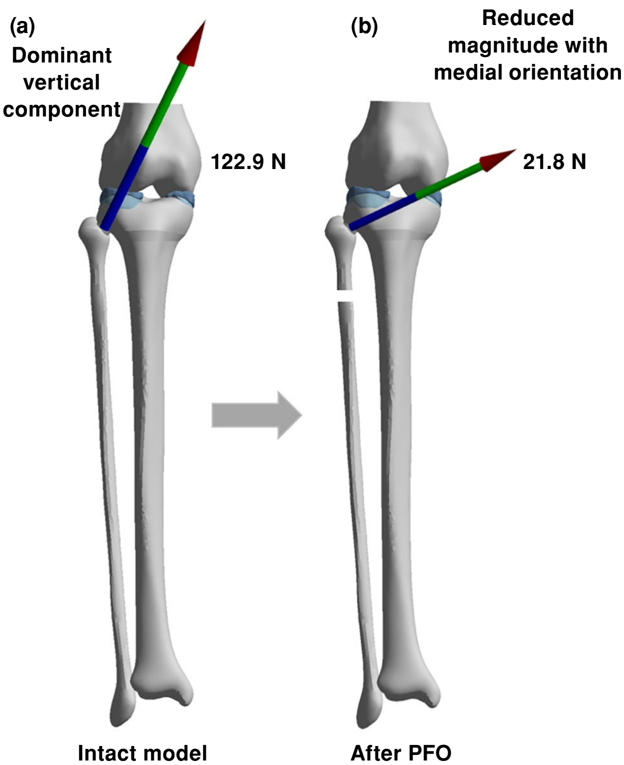

FIGURE 3. Proximal tibiofibular joint reaction force vectors under axial loading: **(a)** intact model showing a dominant vertical force component (122.9 N); **(b)** after PFO, showing reduced force magnitude (21.8 N) and a more medially oriented reaction vector.
PFO, proximal fibular osteotomy.

In the neutral alignment, PFO resulted in only a minimal reduction in medial compartment loading (519.10 N to 514.08 N), with negligible change in the lateral compartment (426.76 N to 424.97 N), indicating limited influence on overall tibiofemoral load distribution. In contrast, PFO produced a pronounced reduction in PTFJ contact force, which decreased from 122.94 N in the intact model to 21.84 N following osteotomy. Vector analysis revealed that, while the force was predominantly vertically oriented in the intact model, it became reduced in magnitude and shifted toward a more horizontal, medially directed orientation after PFO (Figure 3).

To further characterize load redistribution following PFO, distal tibiotalar reaction forces were additionally evaluated. Under neutral alignment, tibiotalar reaction force increased from 787.55 N in the intact model to 897.89 N after osteotomy, while medial and lateral tibiofemoral contact forces remained nearly unchanged. These findings indicate that the reduction in proximal fibular load transmission was predominantly redistributed through distal load-transfer pathways rather than through increased tibiofemoral contact loading.

With increasing varus deformity, tibiofemoral load distribution shifted progressively toward the medial compartment. Medial compartment forces increased to 572.53 N at 3° varus and 608.45 N at 5° varus, whereas lateral compartment forces decreased to 371.48 N and 335.27 N, respectively (Figure 4).

Although PFO consistently reduced PTFJ loading across all deformity levels (from 126.27 N to 22.76

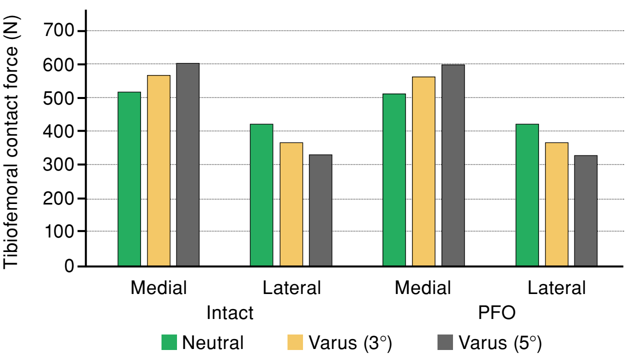

FIGURE 4. Medial and lateral tibiofemoral contact forces under neutral and varus alignment conditions with and without PFO.
PFO, proximal fibular osteotomy.

TABLE IV
Tibiofemoral contact forces and proximal/distal reaction forces under neutral and varus alignment conditions before and after PFO

Model	Medial force (N)	Change (%)	Lateral force (N)	Change (%)	PTFJ force (N)	Change (%)	Distal reaction (N)
Neutral	519.10	–1.0	426.76	–0.1	122.94	–82.2	787.55
Neutral + PFO	514.08		424.97		21.84		897.89
3° Varus	572.53	–0.8	371.48	–0.2	126.27	–82.0	776.39
3° Varus + PFO	567.70		370.82		22.76		896.22
5° Varus	608.45	–0.8	335.27	–0.3	128.38	–82.0	767.99
5° Varus + PFO	603.78		334.42		23.12		894.32

PFO, proximal fibular osteotomy; PTFJ, proximal tibiofibular joint.

N at 3° varus and from 128.38 N to 23.12 N at 5° varus), only minimal changes were observed in tibiofemoral compartment forces (Table IV). Medial compartment force remained elevated under varus conditions (567.70 N at 3° varus and 603.78 N at 5° varus following PFO).

Similarly, distal tibiotalar reaction forces increased after PFO under varus alignment, rising from 776.39 N to 896.22 N at 3° varus and from 767.99 N to 894.32 N at 5° varus. Across all alignment conditions, PFO reduced PTFJ force by approximately 82% while producing less than 1% change in medial tibiofemoral contact force, indicating that the primary biomechanical consequence of osteotomy was redistribution of load transfer within the fibular-ankle pathway rather than unloading of the medial compartment (Table IV).

von Mises stress distributions on the menisci and articular cartilage

Across all loading conditions, stress concentrations were consistently higher in the medial compartment than in the lateral side. In the neutral alignment, peak von Mises stress on the medial meniscus was 7.96 MPa. Following PFO, medial meniscal stress remained largely unchanged at 8.15 MPa (Figure 5).

With progressive varus alignment, peak von Mises stress within the medial meniscus increased markedly, reaching 8.90 MPa at 3° varus and

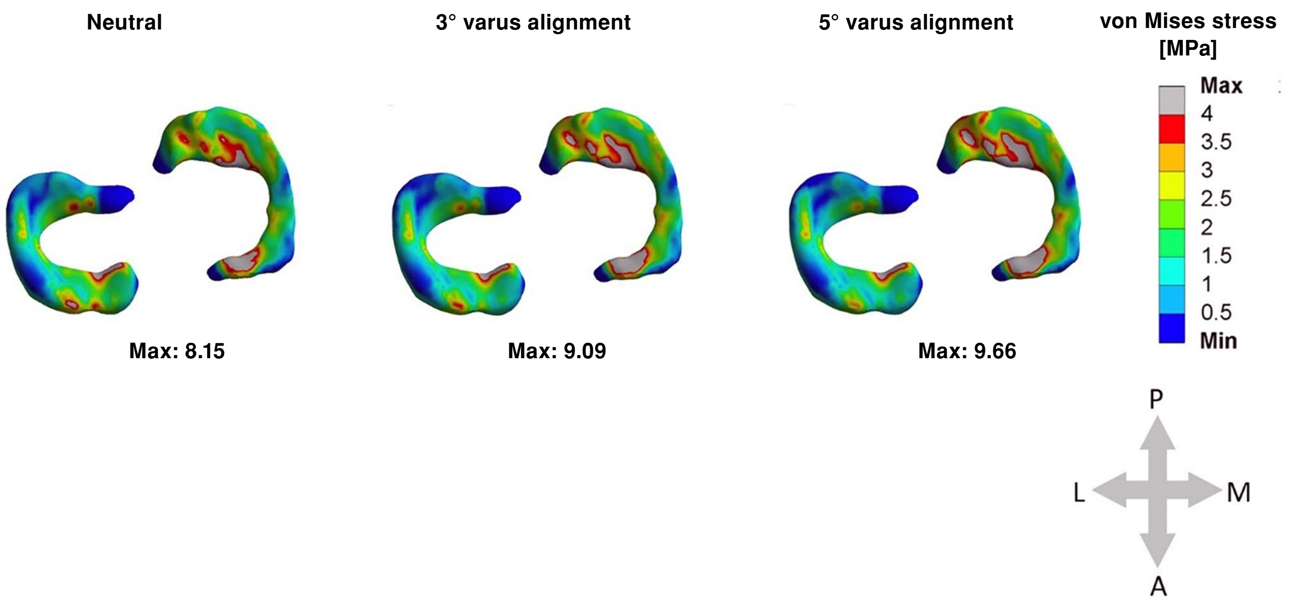

FIGURE 5. von Mises stress distribution in the medial and lateral menisci under neutral, 3° varus, and 5° varus alignment conditions after PFO.
PFO, proximal fibular osteotomy.

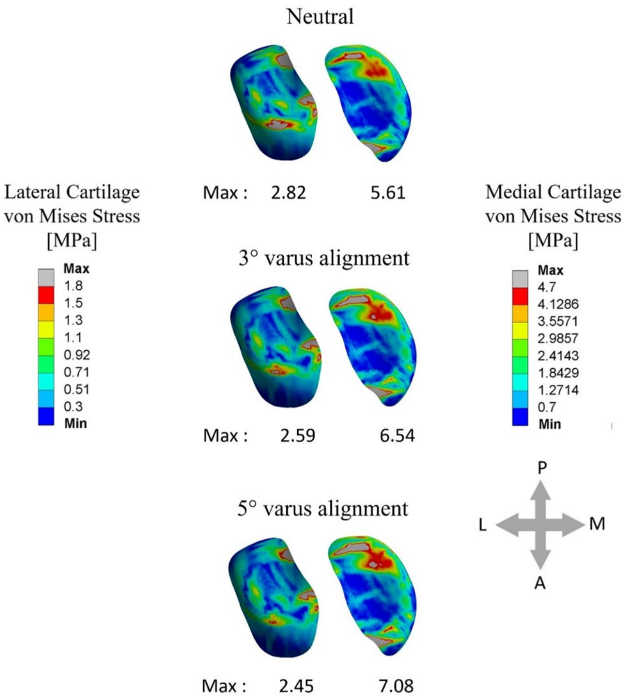

FIGURE 6. von Mises stress distribution in tibial articular cartilage under neutral, 3° varus, and 5° varus alignment conditions after PFO.
PFO, proximal fibular osteotomy.

9.47 MPa at 5° varus. Following PFO, no meaningful reduction was observed in medial meniscal stress under varus conditions (9.09 MPa at 3° varus and 9.66 MPa at 5° varus), indicating limited influence of osteotomy on stress redistribution within the meniscus.

A similar pattern was observed in tibial cartilage. Medial cartilage stress increased from 5.70 MPa under neutral alignment to 6.55 MPa at 3° varus and 7.12 MPa at 5° varus. Following PFO, only minimal changes were observed (6.54 MPa and 7.08 MPa, respectively), whereas lateral cartilage stresses remained comparatively low across all conditions (Figure 6).

DISCUSSION

In the present study, we evaluated the biomechanical consequences of PFO under progressively increasing varus alignment using a lower-extremity FEA framework. The principal finding was that PFO consistently altered load transfer through the fibular pathway, but produced only limited changes in tibiofemoral load distribution across all simulated alignment conditions. Although PTFJ force decreased substantially after osteotomy, medial compartment loading and stress patterns remained largely unchanged, particularly as varus alignment increased. These findings suggest that the biomechanical effects of PFO are primarily confined to the lateral support structures and that the procedure alone may be insufficient to meaningfully unload the medial tibiofemoral compartment in knees with severe varus deformity.

The biomechanical rationale of PFO is commonly linked to the non-uniform settlement theory, which proposes that reducing lateral column support may redistribute load away from the medial compartment.[1,3] Supporting this concept, previous FEA studies have demonstrated reductions in medial tibial cartilage stress and partial load transfer toward the lateral compartment following PFO,[4,6] and clinical studies have reported favorable outcomes, particularly in early-stage OA.[2] Similarly, Ari et al.[8] reported reduced medial compartment stress and posterior load redistribution under axial loading conditions in an intact knee model.

The findings of the present study only partially support this proposed mechanism. Across all simulated alignment conditions, PFO produced a marked reduction in PTFJ force (approximately 82%), confirming that osteotomy substantially modifies load transmission through the fibular pathway.[9] However, medial tibiofemoral contact forces changed by less than 1%, and stress patterns within the meniscus-cartilage complex remained largely preserved. This pattern suggests that the PTFJ and the medial compartment, while anatomically proximate, may operate under largely independent mechanical determinants within the assumptions of the present model. Previous studies have suggested that fibular stability influences load mechanics at both proximal and distal articulations,[2,10] and our kinetic chain model corroborates this view while also revealing the limited influence of isolated fibular unloading in the presence of pronounced axial malalignment.[11] These observations suggest that, within the assumptions of the present model, local unloading of the fibular column does not necessarily translate into proportional unloading of the medial tibiofemoral compartment.

An additional observation that may help explain this behavior was obtained from the evaluation of distal reaction forces. Under neutral alignment, reduction of PTFJ force after PFO was accompanied by an increase in distal tibiotalar reaction force, whereas medial and lateral tibiofemoral contact forces remained nearly unchanged. This finding supports maintenance of global force equilibrium within the FEA system, suggesting that the altered load pathway after osteotomy was redistributed predominantly through distal structures rather than transferred directly to the tibiofemoral compartments. Similar trends were observed under varus alignment conditions. Therefore, the biomechanical effect observed in the present model appears to reflect modification of fibular load transmission rather than direct medial compartment unloading.

Progressive varus alignment remained the dominant factor associated with increased medial compartment loading. Medial meniscal and cartilage stresses increased progressively with worsening varus alignment and persisted after osteotomy. Elevated meniscal stress has previously been associated with mechanically induced nociceptive stimulation and altered joint biomechanics.[12] Proximal fibular osteotomy failed to attenuate these elevated stress concentrations to any meaningful degree, reinforcing the view that fibular unloading, however effective at the PTFJ level, cannot compensate for the stress consequences of a deviated mechanical axis. These findings add biomechanical weight to the growing clinical consensus that procedures directly targeting mechanical axis correction, rather than isolated lateral column decompression, may offer more durable protection of the medial compartment in patients with advanced varus alignment.[13-15]

On the other hand, these findings should be interpreted within the broader context of existing clinical evidence. Proximal fibular osteotomy has demonstrated favorable outcomes in selected patient populations and remains an established surgical option in specific clinical settings.[16] At the same time, previous studies have suggested that biomechanical and clinical outcomes may vary according to alignment severity and overall mechanical environment.[13,17] Of note, the present results do not evaluate clinical effectiveness and should not be interpreted as evidence against the use of PFO. Rather, they demonstrated that, within this simplified biomechanical framework, the effects of PFO were primarily observed in fibular load transfer pathways and were not associated with substantial reductions in medial compartment loading.

An important consideration is that the present model was not intended to reproduce the full complexity of osteoarthritic knee mechanics, but rather to isolate the effect of fibular discontinuity under controlled coronal malalignment conditions. Clinical knees undergoing PFO frequently exhibit additional features including cartilage degeneration, meniscal extrusion, ligament adaptation, joint-line obliquity, and altered gait mechanics, none of which were incorporated into the present analysis. Consequently, the findings should be interpreted as comparative biomechanical observations intended to generate hypotheses regarding load transfer mechanisms rather than direct clinical recommendations.

Nonetheless, the present study has several limitations that should be acknowledged. First, the analysis was based on a single healthy volunteer model; therefore, interindividual anatomical variability and osteoarthritic morphological changes were not represented. In addition, no cadaveric, experimental, or *in vivo* validation was performed. Accordingly, the present findings should be interpreted as comparative biomechanical observations derived from a subject-specific numerical framework rather than direct clinical recommendations. Second, the simulated varus alignment was generated by controlled coronal plane angular rotation and may not fully reproduce the complex multiplanar deformities, joint-line obliquity, cartilage degeneration, and ligamentous adaptations observed in clinical varus knee OA. Third, static axial loading and simplified boundary conditions did not incorporate dynamic muscle forces, ground reaction forces, or gait-cycle-dependent loading conditions.[7,8] Although the model included the ankle-foot complex and preserved global load transfer throughout the lower extremity, the simulated loading condition remains a simplified representation of physiological weight-bearing. Fourth, all anatomical components were modeled using homogeneous, isotropic, and linearly elastic material properties. In particular, the menisci and articular cartilage were represented using simplified constitutive assumptions that did not reproduce the anisotropic, depth-dependent, viscoelastic, and time-dependent mechanical behavior of native tissues, particularly under pathological conditions. These assumptions were intentionally adopted to maintain numerical stability and computational feasibility within the full lower-extremity FEA framework incorporating multiple contact interfaces and ligamentous structures. Therefore, absolute stress magnitudes should be interpreted cautiously, while comparative trends across simulated conditions are expected to remain more robust. Future studies incorporating subject-specific cohorts, experimental validation, and advanced constitutive formulations such as hyperelastic or poroelastic tissue models may provide more physiologically realistic predictions of joint mechanics.

In conclusion, within the constraints of this single-subject static FEA model, PFO consistently reduced PTFJ loading, but produced only limited changes in tibiofemoral load distribution under simulated varus alignment. Although PFO substantially decreased load transfer through the fibular pathway, this reduction was accompanied by increased distal tibiotalar reaction forces, suggesting redistribution of load through distal structures while preserving overall force equilibrium. Progressive varus alignment remained associated with increased medial compartment loading and stress concentration regardless of osteotomy. Taken together, these findings indicate that, under the present modeling assumptions, the biomechanical effects of PFO are primarily related to modification of fibular load-transfer pathways rather than meaningful unloading of the medial tibiofemoral compartment. Therefore, the effectiveness of PFO may depend on the underlying mechanical environment and the severity of varus deformity, with limited capacity to counteract the adverse biomechanical consequences of advanced varus malalignment. Further studies incorporating patient-specific models, dynamic loading conditions, and experimental or clinical validation are needed to better define the biomechanical mechanisms of PFO and to identify the patient populations most likely to benefit from this procedure.

Acknowledgements: The authors would like to thank Musa Güngörürler for his valuable contributions to the development of the finite element model and technical support throughout the study.

Data Sharing Statement: The data that support the findings of this study are available from the corresponding author upon reasonable request.

Author Contributions: O.P.: Contributed to the study conception and design, supervised the study, and drafted the manuscript; A.Y.: Contributed to study design, manuscript drafting, and critical revision. Both authors reviewed and approved the final manuscript.

Conflict of Interest: The authors declared no conflicts of interest with respect to the authorship and/or publication of this article.

Funding: The authors received no financial support for the research and/or authorship of this article.

AI Disclosure: The authors declare that artificial intelligence (AI) tools were not used, or were used solely for language editing, and had no role in data analysis, interpretation, or the formulation of conclusions. All scientific content, data interpretation, and conclusions are the sole responsibility of the authors. The authors further confirm that AI tools were not used to generate, fabricate, or 'hallucinate' references, and that all references have been carefully verified for accuracy.

REFERENCES

1. Dong T, Chen W, Zhang F, Yin B, Tian Y, Zhang Y. Radiographic measures of settlement phenomenon in patients with medial compartment knee osteoarthritis. Clin Rheumatol 2016;35:1573-8. doi: 10.1007/s10067-015-3146-0.
2. Wang X, Wei L, Lv Z, Zhao B, Duan Z, Wu W, et al. Proximal fibular osteotomy: A new surgery for pain relief and improvement of joint function in patients with knee osteoarthritis. J Int Med Res 2017;45:282-9. doi: 10.1177/0300060516676630.
3. Yang ZY, Chen W, Li CX, Wang J, Shao DC, Hou ZY, et al. Medial compartment decompression by fibular osteotomy to treat medial compartment knee osteoarthritis: A pilot study. Orthopedics 2015;38:e1110-4. doi: 10.3928/01477447-20151120-08.
4. Kang Y, Kim J, Sim JA, Moon M, Park JC, Cho SH, et al. Stress effect in the knee joint based on the fibular osteotomy level and varus deformity: A finite element analysis study. Bioengineering (Basel) 2023;10:1003. doi: 10.3390/bioengineering10091003.
5. Morales-Avalos JE, Morales-Avalos R, Martínez-Guajardo KV, Perelli S, Monllau JC, Sánchez Egea AJ, et al. In-silico study of the biomechanical effects of proximal-fibular osteotomy on knee joint contact pressure in varus-valgus misalignment. Med Eng Phys 2024;129:104185. doi: 10.1016/j.medengphy.2024.104185.
6. Unal OK, Dagtas MZ, Demir C, Najafov T, Ugutmen E. The effects of proximal fibular osteotomy on the knee and ankle joints: A finite element analysis. Acta Chir Orthop Traumatol Cech 2021;88:313-20.
7. Pan D, TianYe L, Peng Y, JingLi X, HongZhu L, HeRan Z, et al. Effects of proximal fibular osteotomy on stress changes in mild knee osteoarthritis with varus deformity: A finite element analysis. J Orthop Surg Res 2020;15:375. doi: 10.1186/s13018-020-01894-1.
8. Ari B, Canlidinç M, Yaşar N, Gedik MA. In case effects of proximal fibular osteotomy and total knee arthroplasty on load distribution in the human knee: A comparative finite element study. Jt Dis Relat Surg 2026;37:180-9. doi: 10.52312/jdrs.2026.2455.
9. Marchetti DC, Moatshe G, Phelps BM, Dahl KD, Ferrari MB, Chahla J, et al. The proximal tibiofibular joint: A biomechanical analysis of the anterior and posterior ligamentous complexes. Am J Sports Med 2017;45:1888-92. doi: 10.1177/0363546517697288.
10. Sugianto JA, Hadipranata T, Lazarus G, Amrullah AH. Proximal fibular osteotomy for the management of medial compartment knee osteoarthritis: A systematic review and meta-analysis. Knee 2021;28:169-85. doi: 10.1016/j.knee.2020.11.020.
11. Zhai T, Jiang F, Feng W, Chen Z. Anatomy, biomechanics, and clinical advances of proximal tibiofibular joint in pain management. Front Surg 2025;12:1604538. doi: 10.3389/fsurg.2025.1604538.
12. Daszkiewicz K, Łuczkiewicz P. Biomechanics of medial meniscus tears in the context of pain: A finite element analysis. Front Bioeng Biotechnol 2026;13:1693500. doi: 10.3389/fbioe.2025.1693500.

13. Gultac E, Can Fİ, Hürriyet Aydoğan N. Proximal partial fibular resection versus high tibial osteotomy: Comparative outcomes in early-stage knee osteoarthritis. Jt Dis Relat Surg 2025;36:266-71. doi: 10.52312/jdrs.2025.2107.
14. Liu B, Chen W, Zhang Q, Yan X, Zhang F, Dong T, et al. Proximal fibular osteotomy to treat medial compartment knee osteoarthritis: Preoperational factors for short-term prognosis. PLoS One 2018;13:e0197980. doi: 10.1371/journal.pone.0197980.
15. Morales Avalos JE, Morales-Avalos R, Martínez-Guajardo KV, Pacheco-García LM, Perelli S, Monllau JC, et al. How effective is proximal fibular osteotomy in redistributing joint pressures? Insights from an HTO comparative in-silico study. J Orthop Surg Res 2024;19:333. doi: 10.1186/s13018-024-04807-8.
16. Fu C, Wang F, Zhu Y, Li G, Yuwen P, Wu D, et al. Severe medial osteoarthritis predicts patient dissatisfaction after proximal fibular osteotomy: A mid- to long-term follow-up study. Int Orthop 2024;48:95-101. doi: 10.1007/s00264-023-06036-w.
17. Yapıcı F. High Tibial Osteotomy (HTO), Unicompartmental Knee Arthroplasty (UKA), and Proximal Fibular Osteotomy (PFO) for medial-compartment knee osteoarthritis: A narrative review of comparative mechanisms, clinical outcomes, and decision-making. J Clin Med 2025;14:7882. doi: 10.3390/jcm14217882.